JOURNAL OF MATERIALS SCIENCE 32 (1997) 4857–4864

Mechanical alloying synthesis and structural characterization of ternary Ni-Al-Fe alloys

Z. G. LIU*
Department of Production Systems Engineering, Toyohashi University of Technology, Toyohashi, 441, Japan

J. T. GUO, L. Z. ZHOU
Department of Superalloy and Special Casting, Institute of Metal Research, Chinese Academy of Sciences, Shenyang 110015, People's Republic of China

Z. Q. HU
National Key Lab for RSA, Institute of Metal Research, Chinese Academy of Sciences, Shenyang 110015, People's Republic of China

M. UMEMOTO
Department of Production Systems Engineering, Toyohashi University of Technology, Toyohashi, 441, Japan

Ternary Ni-Al-Fe alloys with different Fe additions have been synthesized by mechanical alloying of elemental powder mixtures. The effects of Fe-substitution for Al in an equi-atomic NiAl alloy on the mechanical alloying process and on the final Ni-Al-Fe alloys were investigated experimentally. Lower Fe additions have been found to prolong the milling time prior to explosive formation of the NiAl(Fe) compound, while $\geqslant$15 at % Fe dition has been found not only to eliminate the explosive reaction during milling but ao to produce a Ni-based supersaturated solid solution (the 15 at % Fe addition results in the formation of an amorphous-like phase). The addition of Fe improves the plastic deformation ility of the alloys and hinders the tendency of fracture during milling, resulting in the formation of larger alloy particles. Upon heating, the as-milled samples with lower Fe addition remain as NiAl(Fe) compound, whereas the Ni-based supersaturated solid solutions decompose into a mixture of compounds of β-(Ni, Fe) (Al, Fe) + γ′-$(Ni, Fe)_3Al$. It is suggested that the ternary addition into the binary intermetallic compound might be possible route to improve ductility by forming the dual phase of β + γ′.

1. Introduction

Some ordered intermetallic compounds have been proposed as potential structural materials at elevated temperature due to their high melting temperature, low density, good thermal stability and high creep resistance. The aluminides are of particular interest because of their excellent oxidation resistance, of which the alloys based on NiAl may offer significant advantages because of the attractive combination of the properties listed above. However, the major barrier to the structural application for NiAl is its low ductility and tendency to fracture in a brittle manner at lower temperatures. Many methods have been applied to improve its ductility at room temperature, such as modification of slip system [1], grain refinement [2, 3], grain boundary elimination [4], microalloying with boron, iron and molybdenum, etc. [5, 6], and composite formation by incorporation of a ductile phase [7]. Although there are some reports of plasticity improvement for NiAl single crystal and for polycrystalline rapidly solidified ribbons, the strain to fracture for the polycrystalline materials was only about 2%, still inadequate for most structural applications.

Recently, an attractive approach for improving the ductility at ambient temperature of NiAl polycrystalline materials has been developed. This is the formation of a dual phase structure of β + γ′ or β + (γ + γ′) (β phase, B2 NiAl, and γ′ phase, $L1_2$ Ni_3Al) in the Ni-rich Ni-Al-X ternary alloys. Combined with the advantages of NiAl and Ni_3Al, this type of material has possibilities in structural applications. Among these alloys, alloys containing Fe have been extensively studied. Inoue *et al.* [8] have studied rapidly solidified wires of Ni-30Al-20Fe and Ni-20Al-30Fe, with the structure of a single β′ phase (Ni, Fe) (Al, Fe) compound, with the structure of $L2_0$) and a duplex γ′ ($L1_2(Ni,Fe)_3(Al,Fe)$) plus β′, which show strains to

*Permanent address: National Key Lab of RSA, Institute of Metal Research, CAS, Shenyang, 110015, People's Republic of China

0022–2461 © *1997 Chapman & Hall*

fracture of 5% and 17%, respectively. The improvement of the room temperature ductility was attributed to: grain size refinement, suppression of ordering and suppression of grain boundary segregation. The studies by Guha *et al.* [9] showed that double extruded Ni-20Al-30Fe gave a 22% plastic elongation, while Chen *et al.* [10] reported recently a 21% elongation in a directionally solidified $Ni_{60}Al_{20}Fe_{20}$ alloy. Alloys of Ni-35Al-20Fe, Ni-25Al-18Fe, etc. have also been studied in this regard [11, 12].

A novel process, mechanical alloying (MA) [13], has been introduced into the fabrication and study of intermetallics in recent years [14–17]. Some studies on mechanical alloying of Ni-Al-Fe alloys [18–21] have been reported. Schaffer and co-workers [18, 19] showed that mechanically alloying Ni-30Al-10Fe resulted in the formation of a nanocrystalline mixture of intermetallic compounds of $(Ni, Fe)_3Al + (Ni, Fe)Al$, which has high thermal stability. It was suggested that the dual phase composite may supply a new route to improve the properties of compounds. Koss *et al.* [20] have shown that mechanically alloying Ni-35Al-20Fe and Ni-31AL-15Fe with Y_2O_3 particles also resulted in improvement of the ductility. To date, nanocrystalline materials have been proposed as a possible route to improve the room temperature ductility of intermetallics [22]. Because mechanical alloying is effective in producing nanocrystalline and/or composite alloys, the authors suggest that by combining the alloying effect and the advanced processing method to produce a fine microstructure and/or a composite, a possible route to improve the room ductility of intermetallic compound may be developed. Based on previous work [23], the present paper reports the mechanical alloying and characterization of Ni-Al-Fe alloys at a series of compositions, as an extended work on the study of MA in Ni-Al-Fe ternary alloys.

2. Experimental

The MA of the mixed powders was performed in a SPEX 8000 mixer/mill equipped with a hardened steel container and balls. The particular sizes and purities of Ni, Al and Fe powders were 15, 15 and 60 μm, and 99.95, 99.5 and 99 at %, respectively. The Ni, Al and Fe elemental powders were mixed in an agate mortar at compositions of $Ni_{50}Al_{50-x}Fe_x$ ($X = 5, 10, 15, 20, 25, 30$) before being placed in the container. The weight ratio of ball to powder was 10 to 1. The milling process was protected by an argon atmosphere. A Cambridge S-360 scanning electron microscope (SEM) with energy dispersive analysis by X-rays (EDAX) was used to characterize the morphology and the composition of the resultant powders (the error is $\pm$ 0.5 at %). The samples were embedded into a phenolic resin and ground, polished for microhardness measurement in a Buehler Micromet II microhardness tester (Hv) with 50 g for 10 s. The average value of at least 5 tests was taken as the microhardness of the sample. The as-milled powders were subjected to thermal analysis in a Perkin-Elmer 7 differential scanning calorimeter, at a heating rate of 20 K min^{-1} up to 973 K, under the protection of an argon atmosphere. X-ray diffraction (XRD) analysis was used to detect the structural evolution of powders, in a RIGAKU D/max-r A X-ray diffractometer using CuK_α radiation. The average crystallite sizes of the samples were calculated through the corrected full width at half maximum (FWHM) of the selected peaks. For evaluating the effect of Fe addition on the end products, the lattice parameters of the different phases were also calculated from the position of the peaks (with an error of $\pm$ 0.0002 nm). The contribution of the residual lattice strain will not be discussed as it is mainly caused by the milling process.

3. Results and discussion

3.1. The structural evolution during mechanical alloying of $Ni_{50}Al_{50-X}Fe_X$ ($X = 5, 10, 15, 20, 25, 30$) alloys by XRD

3.1.1. Mechanical alloying of $Ni_{50}Al_{45}Fe_5$ and $Ni_{50}Al_{40}Fe_{10}$

Both mechanical milling processes of $Ni_{50}Al_{45}Fe_5$ and $Ni_{50}Al_{40}Fe_{10}$ are very similar to the mechanical alloying of the stoichiometry $Ni_{50}Al_{50}$. The XRD patterns of $Ni_{50}Al_{45}Fe_5$ after different milling times are shown in Fig. 1 as an example. After the initial milling stage (which results in grain refinement and the introduction of strain, and therefore intimate homogeneous mixing), the explosive reaction of the formation of NiAl(Fe) compound takes place when milling for 104 and 98 min, respectively, which are 17 and 11 min longer than that for $Ni_{50}Al_{50}$. Further milling completes the reaction, and refines the grains in the NiAl(Fe) compound to an average size of about 15 and 13 nm, respectively.

3.1.2. Mechanical alloying of $Ni_{50}Al_{35}Fe_{15}$

The mechanical alloying process of $Ni_{50}Al_{35}Fe_{15}$ is very different from that of $Ni_{50}Al_{45}Fe_5$ and $Ni_{50}Al_{40}Fe_{10}$ alloys, as shown by the XRD patterns in Fig. 2. The unique feature is that the explosive reaction for forming the NiAl(Fe) compound has vanished. The initial 4 h milling induces gradual formation of the NiAl(Fe) compound, of which the (100), (110), (200) and (211) diffraction peaks appear with the visible peaks of residual elemental Ni shifting towards the low angle side (Fig. 2b).

When milling continues to 10 h, the XRD pattern (Fig. 2c) shows no further diffraction peaks of elemental Ni, Al and Fe. The NiAl(Fe) compound is formed almost completely through the interdiffusion of the elements during milling. The substitution of Fe for Al, combined with heavy deformation during milling, decreases the degree of ordering of the NiAl(Fe) compound, indicated by the weakening and the disappearance of the superlattice diffraction peaks. The average grain size of the NiAl(Fe) compound was measured to be about 10 nm.

When milling is extended to 30 h, the XRD pattern (Fig. 2d) of the sample exhibits an "amorphous-like" appearance. There are only two peaks of the NiAl(Fe) compound, of which the stronger is at $2\theta = 44$ deg, and the weaker at a higher angle is very diffuse. An

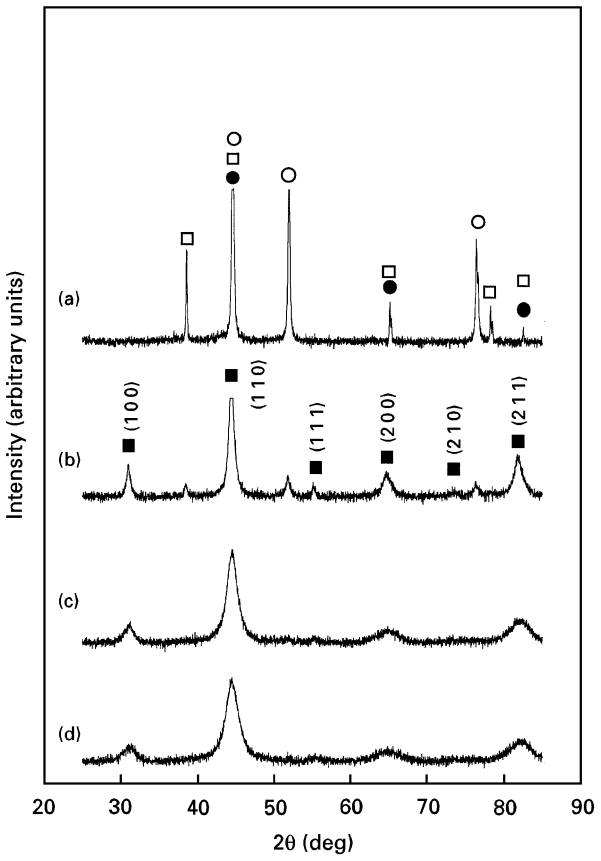

Figure 1 XRD patterns of the $Ni_{50}Al_{45}Fe_5$ alloy after milling (a) 0 h (as-mixed), (b) 105 min (as-exploded), (c) 5 h, and (d) 20 h. (○ Ni, □ Al, ● Fe, ■NiAl(Fe) compound).

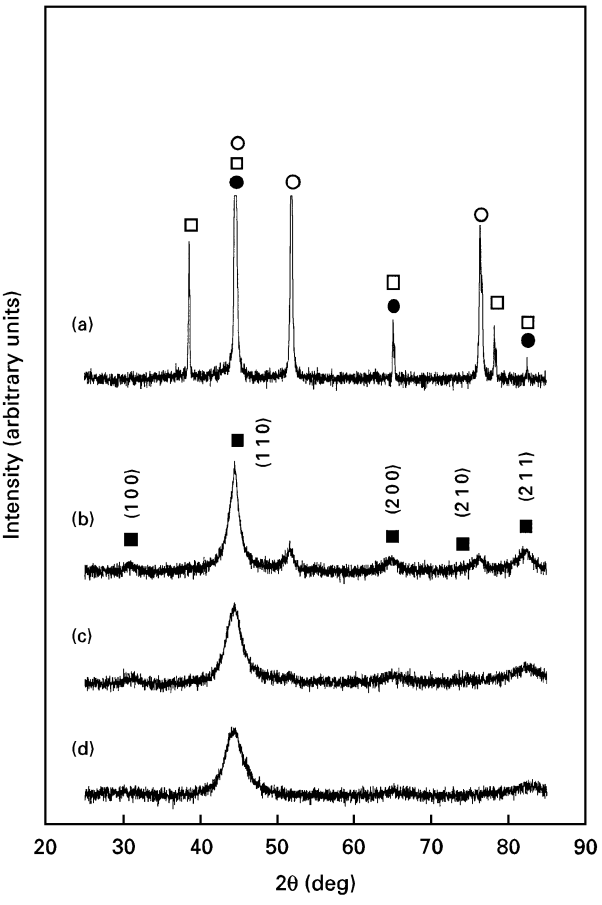

Figure 2 XRD patterns of the $Ni_{50}Al_{35}Fe_{15}$ alloy after milling (a) 0 h (as-mixed), (b) 4 h, (c) 10 h, and (d) 20 h. (○ Ni, □ Al, ● Fe, ■ NiAl(Fe) compound).

evident difference from the typical diffuse peak of the amorphous phase is that the (110) peak is a little sharper, indicating the existence of a mixture of very fine crystalline grains and amorphous phases of the NiAl(Fe) compound.

The previous investigation on mechanical alloying of the Ni-Al-Ti ternary system [23] has shown that the addition of 25 at % Ti eliminates the explosive formation of the NiAl(Ti) compound and induces the formation of an "amorphous-like" phase. Adding 15 at % Fe shows a similar effect to that of adding 25 at % Ti indicating that Fe addition has a more significant effect than Ti addition. It is suggested that the elimination of the explosive reaction is mainly attributed to a decrease in the driving force [23], the heat of formation of the NiAl(Fe) compound. The values of heat released on formation of NiAl and NiTi compounds are $117.5 \pm 8.4\ kJ\ mol^{-1}$ and $67.7\ kJ\ mol^{-1}$ [24], respectively. However, there only exists a solid solution instead of an intermetallic compound in the Ni-Fe binary system, the heat of mixing of $Ni_{50}Fe_{50}$ at 1200 K is only $7.7 \pm 0.8\ kJ\ mol^{-1}$. When Fe is added to NiAl to substitute for Al, a part of the Ni-Al bonding is substituted by Ni-Fe bonding, and the tendency to form a Ni-based solution becomes much stronger than that of forming the NiAl(Fe) compound. Therefore, the heat of formation of the compound decreases significantly. This has been proved by a previous study which showed that MA of the Ni-Fe system significantly extends the composition range of the Ni-Fe solid solution [25]. Hence, explosive formation of the NiAl(Fe) compound will not be able to take place due to a sharp decrease in the driving force.

3.1.3. Mechanical alloying of $Ni_{50}Al_{50-x}Fe_x$ ($X = 20, 25, 30$)

A new phenomenon appears during mechanically alloying of the Ni-Al-Fe ternary system with further Fe addition.

Fig. 3 shows the XRD patterns of a milled $Ni_{50}Al_{25}Fe_{25}$ powder mixture. The explosive formation of the NiAl(Fe) compound was not observed. Instead, a Ni(Al, Fe) supersaturated solid solution (abbreviated as s.s.s.) formed. After 4 h of milling, a trace of the NiAl(Fe) compound formed, indicated by the appearance of the relatively stronger diffraction peak at $2\ \theta = 82.5$ deg, which should be the (211) diffraction of the NiAl(Fe) compound (Fig. 3b). Meanwhile, the positions of the Ni peaks show a shift to lower angles, indicating a solution of Al atoms in a Ni matrix ($r_{Al} = 0.1432$ nm, $r_{Ni} = 0.1248$ nm). After milling for 8 h, the (111) diffraction peak of Ni(Al, Fe) (s.s.s.) becomes even stronger than the (200) peak of Ni (Fig. 3c), indicating a rapid increase of the amount of Ni(Al, Fe) (s.s.s.). After milling for 20 h, the powder mixture transformed completely into Ni(Al, Fe) (s.s.s.) (Fig. 3d).

The mechanical alloying of $Ni_{50}Al_{30}Fe_{20}$ and $Ni_{50}Al_{20}Fe_{30}$ shows similar results to that of $Ni_{50}Al_{25}Fe_{25}$. The difference is that the larger the Fe addition, the higher the supersaturated solid solution formation rate. $Ni_{50}Al_{20}Fe_{30}$ can transform into Ni(Al, Fe) (s.s.s.) completely after milling for 8 h.

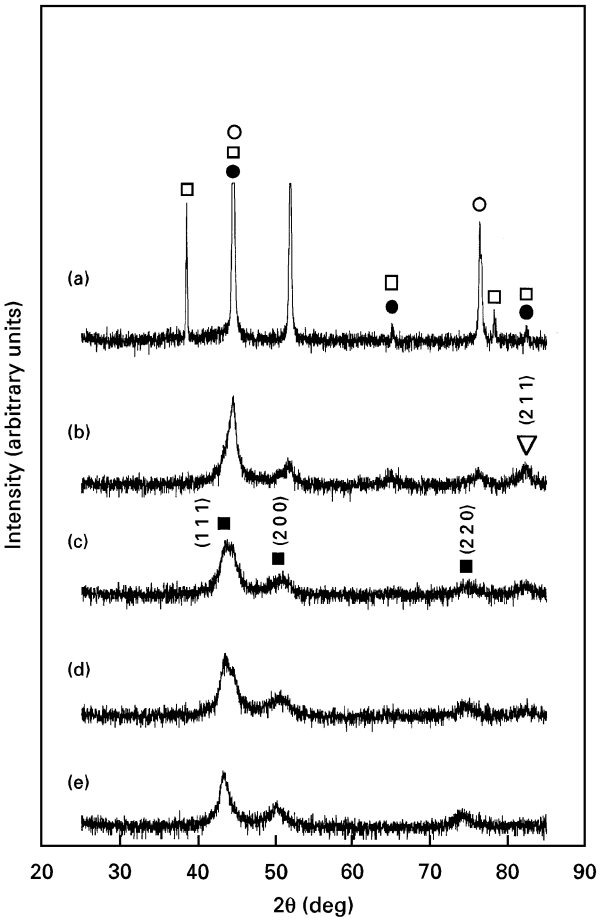

Figure 3 XRD patterns of the $Ni_{50}Al_{25}Fe_{25}$ alloy after milling (a) 0 h (as-mixed), (b) 4 h, (c) 8 h, and (d) 10 h, and (e) 20 h. (○ Ni, □ Al, ● Fe, ■ NiAl(Fe) s.s.s. ∇ NiAl(Fe) compound).

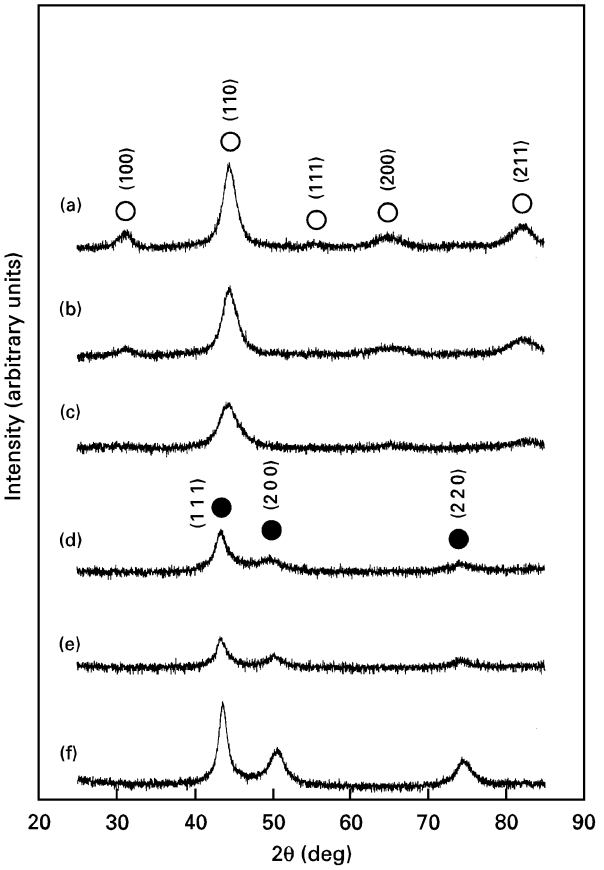

Figure 4 XRD patterns of the final products of $Ni_{50}Al_{50-X}Fe_X$, when $X =$ (a) 5, (b) 10, (c) 15, (d) 20, (e) 25, and (f) 30. (○ NiAl(Fe) compound, ● Ni(Al, Fe) s.s.s.

3.2. The characterization of the resultant products

3.2.1. Comparison of the final products

The effect of Fe addition on the final products is shown in Fig. 4 by XRD patterns of mechanical alloyed $Ni_{50}Al_{50-x}Fe_x$ powders. Both 5 and 10 at % Fe additions have been found to result in the formation of the NiAl(Fe) compound. However, the (111) and (210) peaks of the NiAl(Fe) compound with 10 at % Fe disappear, and the (200) diffraction peak almost disappears as well compared to that of the 5 at % Fe addition sample. This is attributed to; (a) the addition of Fe reduces the degree of order, and (b) the existence of very fine crystalline grains. The 15 at % Fe addition has been found to induce the formation of an amorphous-like phase. It is deduced to be the coexistence of an amorphous phase and a very fine NiAl(Fe) compound and/or Ni(Al, Fe) (s.s.s.) crystals (Fig. 4c). For $\geqslant 20$ at % Fe addition the final product is disordered Ni(Al, Fe) (s.s.s.) (Fig. 4d–f). This phenomenon is different from that of the equilibrium state. Fig. 5 is the equilibrium Ni-Al-Fe phase diagram [26]. It is shown that the $Ni_{50}Al_{50-x}Fe_x$ alloy remains as β-(Ni, Fe) (Al, Fe) phase when X is <20, and $\beta + \gamma$ (Fe, Ni) phases occur when X is 21–37, independent of temperature. It is argued that the formation of Ni(Al, Fe) (s.s.s.) instead of $\beta + \gamma$ dual phases for larger Fe additions is due to the heavy deformation during milling kinetically favouring the formation of a disordered structure. The most readily formed should be the Ni-based solid solution. That is also in good agreement with the previous results on the composition extension of solid solutions by MA [27].

Moreover, increasing Fe addition decreases the lattice parameters of the Ni(Al, Fe) (s.s.s.) compound. The lattice parameters of Ni(Al, Fe) (s.s.s.) of $Ni_{50}Al_{50-x}Fe_x$ ($X = 20, 25, 30$) are measured to be 0.3612 nm, 0.3611 nm and 0.3607 nm, respectively. It is easy to understand that larger amounts of the smaller Fe atoms, together with reduced amounts of the larger Al atoms, results in the reduction of the lattice parameter. The average crystalline grain sizes of the Ni(Al, Fe) (s.s.s.) are measured to be 5 nm, 6 nm and 7 nm, respectively (see Table I).

3.2.2. The morphology of the resultant products

The morphology of the as-milled final products of the Ni-Al-Fe ternary alloys is also significantly affected by the various Fe additions (Fig. 6).

The explosively formed NiAl(Fe) compounds of $Ni_{50}Al_{45}Fe_5$ and $Ni_{50}Al_{40}Fe_{10}$ show very fine and homogeneous particles with an average size of 1–2 μm and 3–4 μm, respectively, which is very close to that of the NiAl particles without Fe addition [15], denoting

the absence of plastic deformation. When Fe addition increases to 15 at %, the particle of the amorphous-like phase becomes a little larger, 4–10 μm, with decreasing uniformity.

The morphology of the Ni(Al, Fe) (s.s.s.) powders is very different. The particle size is much larger than that of the explosively formed NiAl compound. Ni(Al, Fe) (s.s.s.) of 20, 25 and 30 at % Fe addition show particle sizes of 20–60, 50 and 60–70 μm, respectively. On the other hand, the surface characteristic of the powder particles is also changed. The Ni(Al, Fe) (s.s.s.) powder particles reveal much more plastic deformation during mechanical milling, which is indicated by the obvious pullout burrs and/or push-down hollows on the surface of the particles. Both the increase in particle size with increasing Fe addition and the obvious characteristics of plastic deformation of the solid solution particles imply that the addition of Fe actually improves the ductility of the samples. Therefore, the addition of Fe facilities cold-welding and hinders fracture during mechanical milling, resulting in larger powder particles. These results are in agreement with the viewpoint that Fe is a ductilizing element for NiAl intermetallics [25].

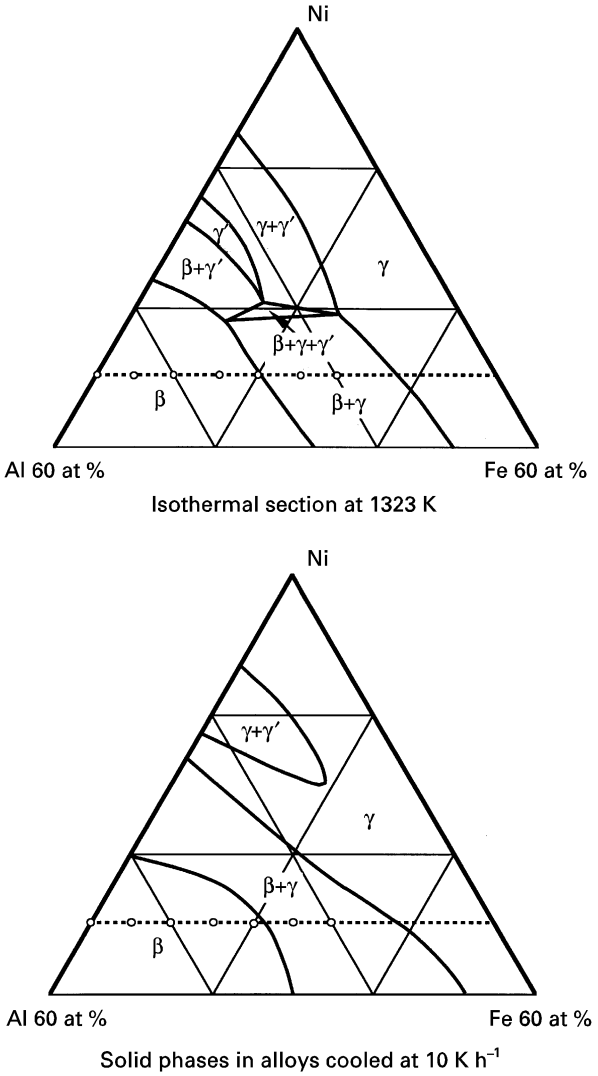

Figure 5 The phase diagram of the Ni-Al-Fe ternary alloy [26]. The open circles indicate the alloy composition in the text.

The composition of the samples was also analysed by EDAX (see Table I). The analytical compositions of the final products are all very close to the starting nominal values. A slightly higher Fe content was due to milling media debris (mainly Fe) mixed into the alloys during milling.

3.2.3. Microhardness measurement of the final products

The microhardness was measured to characterize the mechanical properties of the resultant powders. The measurements reveal that the addition of Fe decreases the microhardness of the alloys (Fig. 7, also see Table I). Addition of 5 at % Fe sharply decreases the microhardness of the NiAl(Fe) compound to 741 Hv, from 846 Hv for NiAl. The NiAl(Fe) compound containing 10 at % Fe shows a microhardness of 736 Hv, almost the same as that of a NiAl(Fe) compound with 5 at % Fe. The "amorphous-like" phase with 15 at % Fe addition gives a value of 707 Hv, a little lower than that of the NiAl(Fe) compound. The microhardness decreases further with increasing Fe, to 650–677 Hv for Ni(Al, Fe) (s.s.s.). It is clear that increasing Fe decreases the hardness of the alloys whereas it improves their ability to plastically deform. This is in good agreement with the morphology observations.

TABLE I Analysis of the as-milled $Ni_{50}Al_{50-X}Fe_x$ powders

Sample	$Ni_{50}Al_{45}Fe_5$	$Ni_{50}Al_{40}Fe_{10}$	$Ni_{50}Al_{35}Fe_{15}$	$Ni_{50}Al_{30}Fe_{20}$	$Ni_{50}Al_{25}Fe_{25}$	$Ni_{50}Al_{20}Fe_{30}$
End Products Composition (at %)	NiAl(Fe)	NiAl(Fe)	Ni(Al,Fe)am	Ni(Al,Fe)	Ni(Al,Fe)	Ni(Al,Fe)
Ni	51.8	51.9	51.5	49.7	48.3	48.0
Al	42.3	36.8	31.2	27.1	23.9	19.5
Fe	5.9	11.3	17.3	23.2	27.8	32.5
Total	100	100	100	100	100	100
Microhardness, (Hv)	741	736	707	675	650	677
Average crystal size, (nm)	15	13	—	5	6	7

*am- "amorphous-like" phase.

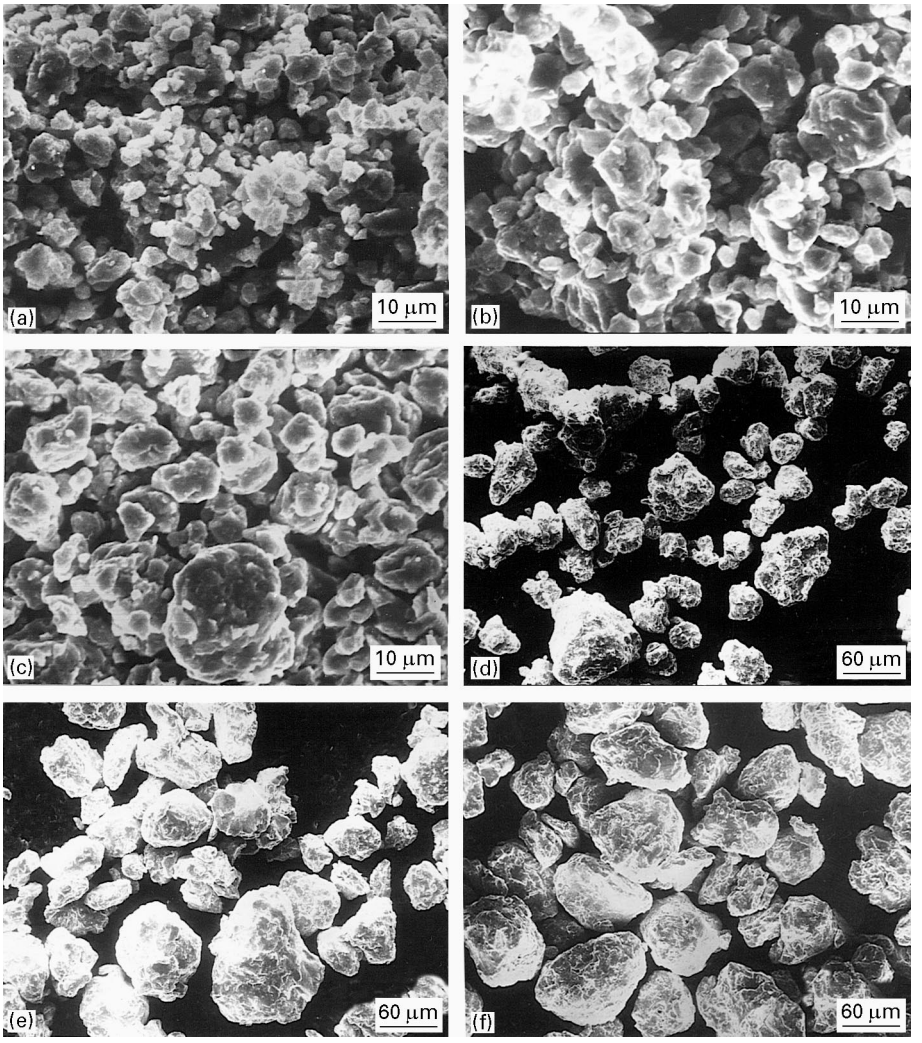

Figure 6 SEM micrographs of the final products of $Ni_{50}Al_{50-x}Fe_x$, when $X =$ (a) 5, (b) 10, (c) 15, (d) 20, (e) 25, and (f) 30. The change in particle sizes and the characteristics of the particle surface is indicative of the increase of the deformability of the powder particles.

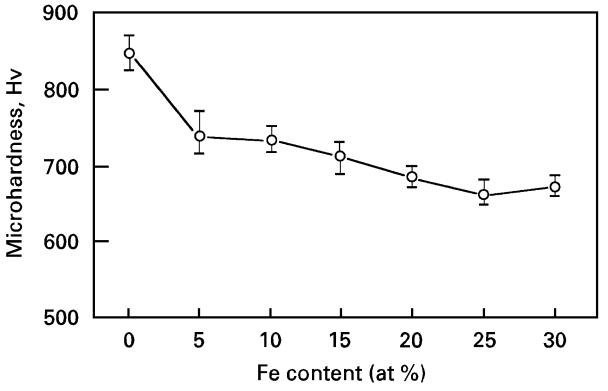

Figure 7 Microhardness of the as-milled $Ni_{50}Al_{50-x}Fe_x$ powders as a function of composition. This clearly shows the decrease of the hardness with increasing Fe addition and the change of the products.

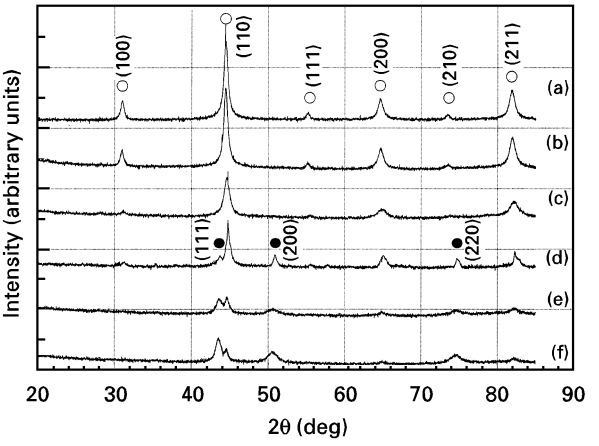

Figure 8 XRD patterns of the final products of $Ni_{50}Al_{50-x}Fe_x$ after heating to 973 K, when $X =$ (a) 5, (b) 10, (c) 15, (d) 20, (e) 25, and (f) 30. ○-β (Ni, Fe) (Al, Fe), ●-γ′$(Ni, Fe)_3Al$.

3.2.4. Thermal analysis of the as-milled Ni-Al-Fe powders

Thermal analysis was conducted to test the thermal stability of the as-milled Ni-Al-Fe products. The results show a slow heat release during heating of the samples up to 973 K, without any other exo- or endothermal effects. Fig. 8 shows the XRD patterns of the samples after heating. The Ni(Al, Fe) compounds with 5 and 10 at % Fe addition remain unchanged (Fig. 8a and b), while the "amorphous-like" phase with 15 at % Fe also transformed into the Ni(Al, Fe)

TABLE II Characterization of the $Ni_{50}Al_{50-x}Fe_x$ powders after heating to 973 K

Sample		$Ni_{50}Al_{45}Fe_5$	$Ni_{50}Al_{40}Fe_{10}$	$Ni_{50}Al_{35}Fe_{15}$	$Ni_{50}Al_{30}Fe_{20}$	$Ni_{50}Al_{25}Fe_{25}$	$Ni_{50}Al_{20}Fe_{30}$
Lattice parameter (nm)	β-Ni(Al,Fe)	0.2880	0.2879	0.2871	0.2870	0.2871	0.2872
	γ'-$(Ni,Fe)_3Al$	—	—	—	0.3597	0.3595	0.3591
Average crystal size (nm)	β-Ni(Al,Fe)	18	14	11	15	13	10
	γ'-$(Ni,Fe)_3Al$	—	—	—	12	18	22

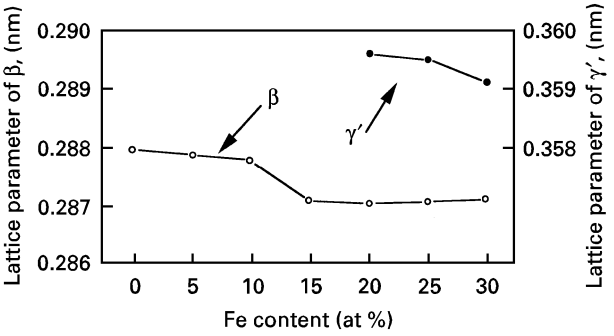

Figure 9 Lattice parameter of β and γ' phases of $Ni_{50}Al_{50-x}Fe_x$ after heating to 973 K.

compound. This is different from the as-milled "amorphous-like" Ni-Al-Ti alloys [28], which showed a two-step transition into the Ni_2AlTi compound upon heating. According to the previous study on the small amount of Fe added into stoichiometric NiAl, the Fe atoms prefer to occupy the Al sites in the lattice of NiAl [29]. However, the larger amount of Fe addition will cause the Fe atoms to occupy the Ni sites because of the similar properties of Fe and Ni. Thus, the compound should be β-(Ni, Fe) (Al, Fe). The measurements of lattice parameters of these NiAl(Fe) compounds show that increasing Fe reduces the lattice parameter of the NiAl(Fe) compounds, which are 0.2879, 0.2878 and 0.2871 nm, respectively, for 5, 10 and 15 at % Fe addition, all of which are smaller than that of NiAl ($a_{NiAl} = 0.2886$ nm). The degree of ordering of the NiAl(Fe) compounds was also found to decrease with increasing Fe addition according to the XRD analysis.

The higher Fe addition disordered Ni(Al, Fe) (s.s.s.) decomposed into a mixture of β and γ' Ni_3Al-type phases during heating. The proportions of the γ' phase in the decomposed products increase with increasing Fe (Fig. 9). Precise measurement shows that with increasing Fe, the lattice parameters of the β phase in the mixture appear to remain almost unchanged (see Table II), while the lattice parameter of the γ' phase decreases sharply, but is still larger than that of the Ni_3Al compound ($a_{Ni_3Al} = 0.3561$ nm).

Further Fe addition is beneficial to the formation of the γ' phase. The measurement of the lattice parameter indicates that more Fe atoms are used to substitute for Ni atoms to form the γ' phase and reduces the lattice parameter of the γ' phase, therefore inducing a slight increase of the lattice parameter of the β phase. It is reasonable to deduce that the γ' phase is the $(Ni, Fe)_3Al$ compound.

Both the β and γ' phases after heating keep the crystallite size at the nanometer scale (see Table II). For the dual phase samples, the crystallite size of the β phase decreases while the crystallite size of the γ' phase increases with increasing Fe addition. This should benefit the ductility of the samples, and further work on this aspect is underway.

4. Summary

Systematic investigations on the mechanical alloying of the ternary Ni-Al-Fe system indicate that the addition of Fe, substituting for Al in NiAl, exerts a great influence on the mechanical alloying process and the final products. The addition of Fe improves the ability of the alloys to plastically deform, reduces the tendency of fracture during milling, and results in the formation of larger alloy particles with crystals in the nanometer range. The Ni(Al, Fe) supersaturated solid solution with higher Fe addition decomposed into a dual-phase mixture of β-(Ni, Fe) (Al, Fe) + γ'-$(Ni, Fe)_3Al$, upon heating. By selecting an appropriate composition and treatment, the appropriate microstructure (i.e., the dual phase of $\beta + \gamma'$) and properties can be achieved. More intensive work on consolidation and improvement of properties is being conducted.

Acknowledgements

The authors wish to acknowledge Mrs X. Z. Zhang and Mr X. P. Song for their work on the X-ray diffraction analysis and for many useful discussions.

References

1. R. D. FIELD, D. F. LAHRMAN and R. DAROLIA, *Acta Metall. Mater.* **42** (1994) 2961.
2. Z. G. LIU, J. T. GUO, N. L. SHI and Z. Q. HU, *J. Mater. Sci. Technol.* **12** (1996) 7.
3. K. J. CHAN, *Scripta Metall.* **24** (1990) 1725.
4. K. VEDULA and P. S. KHADKILUR, in "High Temp. Aluminides and Intermetallics", edited by S. H. Whang, C. T. Liu, D. P. Pope and J. O. Stiegler, (TMS Warrendale, PA, 1990) p. 197.
5. I. BAKER and P. R. MUNROE, *J. Met.* **40** (1988) 28.
6. R. DAROLIA, *ibid.* **43** (1991) 44.
7. V. C. NARKONE, J. R. SRIEF and K. M. PREWE, in "Intermetallic Matrix Composites", edited by D. L. Arton, P. L. Martin, D. B. Miracle and R. McMeeking, (Pittsburgh, PA, 1990) p. 194.

8. A. INOUE, T. MASUMOTO and H. TOMIOKA, *J. Mater. Sci.* **19** (1984) 3097.
9. S. GUHA, P. R. MUNROE and I. BAKER, *Mater. Res. Soc. Symp. Proc.* **133** (1989) 633.
10. J. CHEN, Q. ZHANG, Y. J. TANG and Z. Q. HU, *Mater. Lett.* **22** (1995) 145.
11. D. R. PARK, M. V. NATHAL and D. A. KOSS, *Mater. Res. Soc. Symp. Proc.* **133** (1989) 561.
12. K. ISHIDA, R. KARNUMA, N. UENO and T. NISHIZAWA, *Metall. Trans. A* **22** (1991) 441.
13. J. S. BENJAMIN and T. E. VOLIN, *Metall. Trans.* **5** (1974) 1929.
14. M. ATZMON, *Phys. Rev. Lett.* **64** (1990) 487.
15. Z. G. LIU, J. T. GUO, L. L. HE and Z. Q. HU, *Nanostruct. Mater.* **4** (1994) 87.
16. P. MATTEAZZI and G. LE CAER, *J. Am. Ceram. Soc.* **74** (1991) 1382.
17. S. SRINIVASAN, S. R. CHEN and R. R. SCHWARZ, *Mater. Sci. Eng. A* **153** (1992) 691.
18. G. B. SCHAFFER, *Scripta Metall. Mater.* **27** (1992) 1.
19. G. B. SCHAFFER and A. J. HERON, in Proceedings of the Second International Conference on Mechanical alloying for structural applications, Vancouver, 1993, edited by J. J. deBarbadilo, F. H. Froes and R. Schwarz (ASM Int., Materials Park, OH, 1993) p. 197.
20. D. S. KOSS, J. BREEDIS, L. LOCCI and J. POOLE, *ibid.* p. 275.
21. E. GAFFET, *Nanostruct. Mater.* **5** (1995) 393.
22. R. BOHN, T. HAUBOLD, R. BIRRINGER and H. GLEITER, *Scripta Metall. Mater.* **25** (1991) 811.
23. Z. G. LIU, J. T. GUO and Z. Q. HU, *Mater. Sci. Eng. A* **192/193** (1995) 577.
24. H. SCHROPF, C. KUHRT, E. ARZT and L. SCHWARZ, *Scripta Metall. Mater.* **30** (1994) 1569.
25. C. KUHRT and L. SCHULTZ, *J. Appl. Phys.* **73** (1993) 1975.
26. G. PETZOW and G. EFFENBERG, "Ternary Alloys", Vol. 5, (FRG, VCH, Verlagsgesellschaft, New York, 1992) p. 321.
27. J. ECKERT, J. C. HOLZER and W. L. JOHNSON, *J. Appl. Phys.* **73** (1993) 131.
28. Z. G. LIU, J. T. GUO and Z. Q. HU, *Acta Metall. Sin.* **8** (1995) 583.
29. P. CHARTIER, M. BALASUBRAMANIAN, D. BREWE, T. MANZUR, D. PEASE, J. BUDERICK, L. HUANG, C. LAW, S. RUSELL and C. KIMBALL, *J. Appl. Phys.* **75** (1984) 3842.

Received 14 April 1996
and accepted 11 February 1997